Bridging the gap between hadronic spectroscopy and light-front observables

(lecture 1) hadrons on LF

Edward Shuryak

Center for Nuclear Theory, Stony Brook University

Based on summary book
of 20+papers
with Ismail Zahed
and Nick Miesch
2019-2026
e-Print: 2601.15085

LF lectures, March 2026

The book is very large
(even table of contents is 8 pages)
and highly technical (appendices)
so it cannot be presented in few lectures

QCD vacuum
topology, semiclassics

hadronic spectroscopy
multiquarks, Fermi statistics

Spectroscpy on LF
WF -> PDFs, FFs, GPDs

Project as a bridge

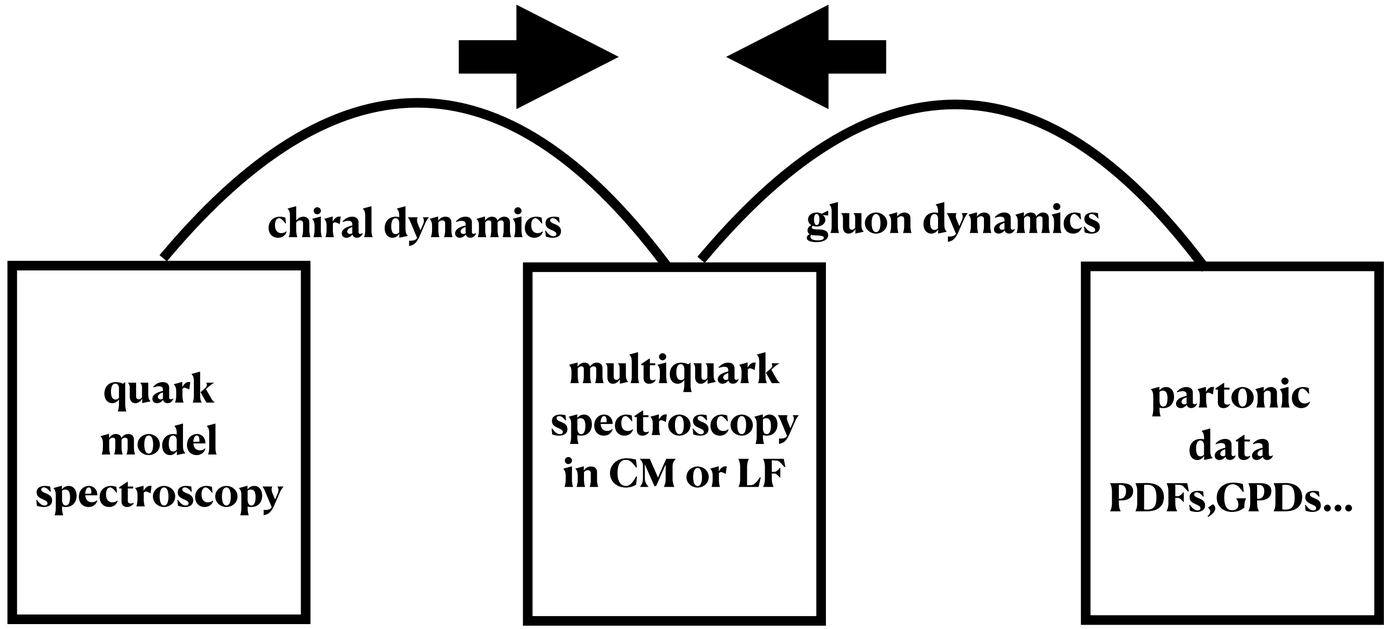

$Q^2 \sim \rho^{-2} \sim 0.4\,GeV^2$ $Q^2 \sim 1\,GeV^2$ $Q^2 \sim 4\,GeV^2$

Why repeat the QCD spectroscopy on the light front?

connection to partonic observables, DA, PDFs,GPDs, formfactors

in the rest frame, nonrelativistic approximation only works
if masses are much larger than momenta,
on the LF p_t^2 appear as a sum with m^2
and it does not matter which one is larger
=> same setting from Upsilons to light quark hadrons

$$m^2 \gg \vec{p}^2 \quad ?$$

kinetic energy on LF

$$\frac{p_{1\perp}^2 + m_Q^2}{x_1} + \frac{p_{2\perp}^2 + m_Q^2}{x_2} + \frac{p_{3\perp}^2 + m_Q^2}{x_3} =$$

Why repeat the QCD spectroscopy on the light front?

connection to partonic observables, DA, PDFs,GPDs, formfactors

in the rest frame, nonrelativistic approximation only works
if masses are much larger than momenta,
on the LF p_t^2 appear as a sum with m^2
and it does not matter which one is larger
=> same setting from Upsilons to light quark hadrons

$$m^2 \gg \vec{p}^2 \quad ?$$

kinetic energy on LF

$$\frac{p_{1\perp}^2 + m_Q^2}{x_1} + \frac{p_{2\perp}^2 + m_Q^2}{x_2} + \frac{p_{3\perp}^2 + m_Q^2}{x_3} =$$

transverse momenta appear quadratic, as usual,
yet longitudinal momenta appear in a complicated manner,
how to do QM with that ?

Philosophy: start with "bare bone" LF Hamiltonian
constituent quarks + confinement
and solve it as accurate as possible,
with no arbitrary assumptions/approximations

no need for "CM motion subtraction"

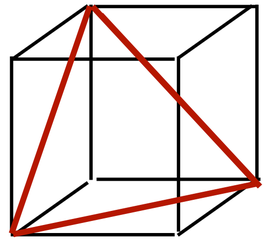

Jacobi coordinates

$$\vec{p}_{1\perp} = (\sqrt{6}\vec{p}_{\lambda\perp} + 3\sqrt{2}\vec{p}_{\rho\perp})/6, \qquad x_1 = (\sqrt{6}\lambda + 3\sqrt{2}\rho + 2X)/6$$
$$\vec{p}_{2\perp} = (\sqrt{6}\vec{p}_{\lambda\perp} - 3\sqrt{2}\vec{p}_{\rho\perp})/6, \qquad x_2 = (\sqrt{6}\lambda - 3\sqrt{2}\rho + 2X)/6$$
$$\vec{p}_{3\perp} = -\sqrt{6}\vec{p}_{\lambda\perp}/3 \qquad x_3 = (-\sqrt{6}\lambda + X)/3$$

$$X = x_1 + x_2 + x_3$$

longitudinal variables
are defined on equilateral triangle

The kinetic part of the LF Hamiltonian

$$\frac{p_{1\perp}^2 + m_Q^2}{x_1} + \frac{p_{2\perp}^2 + m_Q^2}{x_2} + \frac{p_{3\perp}^2 + m_Q^2}{x_3} =$$

$$3\sum_i (p_{i\perp}^2 + m_i^2) + \sum_i (p_{i\perp}^2 + m_i^2)\left(\frac{1}{x_i} - 3\right)$$

transverse
two 2d oscillators

non-factoriwable
"cup potential"

which is mostly zero
except near the edges
forcing LFWFs to vanish

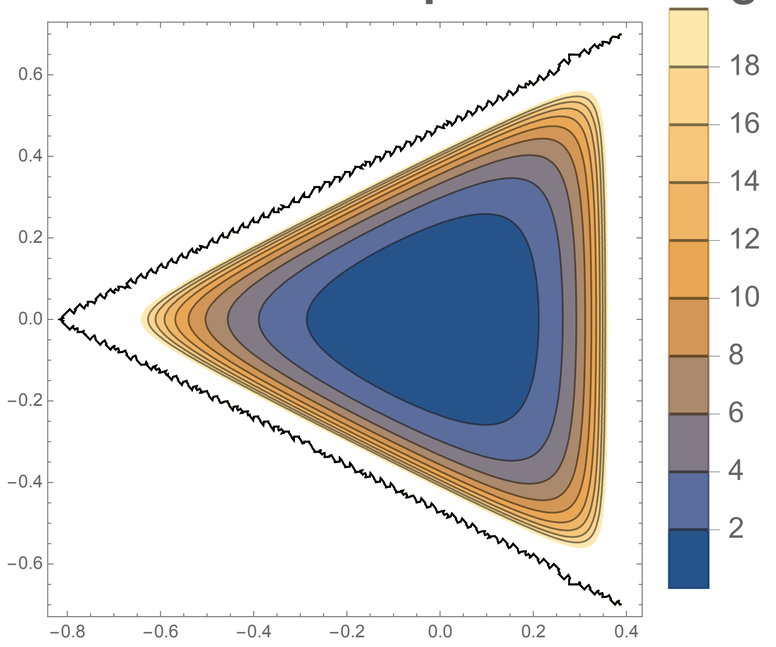

IG. 4. The contour plot of the "triangular cup" pote
al $V(\lambda, \rho)$ on λ, ρ plot.

Confining Hamiltonian on LF can be desribed by:

Nambu-Goto string

$$S[\theta] = \int_0^T d\tau \sum_{i=1}^{3} \left(e_i m_i^2 + \frac{1}{4e_i} \dot{x}_i^2 \right) \qquad (37)$$

$$+\sigma_T \sum_{i=1}^{3} \int_0^T d\tau \int_0^1 d\sigma_i \sqrt{\dot{X}_i^2 X_i'^2 - (\dot{X}_i \cdot X_i')^2}$$

In momentum representation coordinates are derivatives, that is how we get a Laplacian

$$\to \int_0^T d\tau \left(3em_Q^2 + \frac{3}{4e} \right.$$

$$\left. + \frac{1}{4e} (\dot{r_\lambda}^2 + \dot{r_\rho}^2) + \sigma_T \sum_{i=1}^{3} |\xi_i(\theta)| \right)$$

the square root

coord's are derivative over momenta

Confining Hamiltonian on LF can be desribed by:

Nambu-Goto string

$$S[\theta] = \int_0^T d\tau \sum_{i=1}^{3} \left(e_i m_i^2 + \frac{1}{4e_i} \dot{x}_i^2 \right) \qquad (37)$$

$$+\sigma_T \sum_{i=1}^{3} \int_0^T d\tau \int_0^1 d\sigma_i \sqrt{\dot{X}_i^2 X_i'^2 - (\dot{X}_i \cdot X_i')^2}$$

In momentum representation coordinates are derivatives, that is how we get a Laplacian

$$\to \int_0^T d\tau \left(3em_Q^2 + \frac{3}{4e} \right.$$

$$\left. + \frac{1}{4e} (\dot{r_\lambda}^2 + \dot{r_\rho}^2) + \sigma_T \sum_{i=1}^{3} |\xi_i(\theta)| \right)$$

the square root

coord's are derivative over momenta

$$\approx \sum_{i=1}^{3} \left(\frac{k_{i\perp}^2 + m_Q^2}{x_i} \right.$$

$$\left. + \sigma_T \left(3a + \frac{1}{a} \sum_{i=1}^{3} (|i\partial/\partial x_i|^2 + (3m_Q)^2 b_{i\perp}^2) \right) \right)$$

Confining Hamiltonian on LF can be desribed by:

Nambu-Goto string

$$S[\theta] = \int_0^T d\tau \sum_{i=1}^{3} \left(e_i m_i^2 + \frac{1}{4e_i} \dot{x}_i^2 \right) \qquad (37)$$

$$+\sigma_T \sum_{i=1}^{3} \int_0^T d\tau \int_0^1 d\sigma_i \sqrt{\dot{X}_i^2 X_i'^2 - (\dot{X}_i \cdot X_i')^2}$$

In momentum representation coordinates are derivatives, that is how we get a Laplacian

minimization over auxiliary parameter a can be done AFTER the Hamiltonian is diagonalized

$$\to \int_0^T d\tau \left(3em_Q^2 + \frac{3}{4e} \right.$$

$$\left. + \frac{1}{4e} (\dot{r_\lambda}^2 + \dot{r_\rho}^2) + \sigma_T \sum_{i=1}^{3} |\xi_i(\theta)| \right)$$

the square root

coord's are derivative over momenta

$$\approx \sum_{i=1}^{3} \left(\frac{k_{i\perp}^2 + m_Q^2}{x_i} \right.$$

$$\left. + \sigma_T \left(3a + \frac{1}{a} \sum_{i=1}^{3} (|i\partial/\partial x_i|^2 + (3m_Q)^2 b_{i\perp}^2) \right) \right)$$

Philosophy: in momentum representation confinement produces derivative terms leading to Schreodinger-like equation

The Laplacian (which we encounter in the confining term of the Hamiltonian) in the original coordinates also takes a simple form

$$\nabla^2 = \sum_i \frac{\partial^2}{\partial x_i^2} \to \frac{\partial^2}{\partial \lambda^2} + \frac{\partial^2}{\partial \rho^2} + 3\frac{\partial^2}{\partial X^2} \qquad (31)$$

$$\varphi^{Dc}_{m,n}(\lambda,\rho) = \frac{4}{L\,3^{\frac{3}{4}}}\left[\cos\left(\frac{2\pi(2m_L-n_L)\rho}{3L}\right)\sin\left(\frac{2\pi n_L\tilde{\lambda}}{\sqrt{3}L}\right)\right.$$
$$-\cos\left(\frac{2\pi(2n_L-m_L)\rho}{3L}\right)\sin\left(\frac{2\pi m_L\tilde{\lambda}}{\sqrt{3}L}\right)$$
$$\left.+\cos\left(\frac{2\pi(m_L+n_L)\rho}{3L}\right)\sin\left(\frac{2\pi(m_L-n_L)\tilde{\lambda}}{\sqrt{3}L}\right)\right]$$
$$\varphi^{Ds}_{m,n}(\lambda,\rho) = \frac{4}{L\,3^{\frac{3}{4}}}\left[\sin\left(\frac{2\pi(2m_L-n_L)\rho}{3L}\right)\sin\left(\frac{2\pi n_L\tilde{\lambda}}{\sqrt{3}L}\right)\right.$$
$$-\sin\left(\frac{2\pi(2n_L-m_L)\rho}{3L}\right)\sin\left(\frac{2\pi m_L\tilde{\lambda}}{\sqrt{3}L}\right)$$
$$\left.-\sin\left(\frac{2\pi(m_L+n_L)\rho}{3L}\right)\sin\left(\frac{2\pi(m_L-n_L)\tilde{\lambda}}{\sqrt{3}L}\right)\right] \qquad (54)$$

with $\tilde{\lambda} = \lambda + L/\sqrt{3}$. Their symmetry properties include e.g. ρ mirror symmetry

$$\varphi^{Dc,s}_{m_L,n_L}(\lambda,-\rho) = \pm\varphi^{Dc,s}_{m_L,n_L}(\lambda,\rho) \qquad (55)$$

Full set of Eigenfunctions of the Laplacian on the equilateral triangle can be found both analytically (6 standing waves) and numerically with Mathematica

The Dirichlet states with $m_L = 2n_L$ are non-degenerate, with normalized eigenstates [14]

$$\varphi^{D}_{2n_L,n_L}(\lambda,\rho) =$$
$$\frac{2^{\frac{3}{2}}}{L\,3^{\frac{3}{4}}}\left[2\cos\left(\frac{2\pi n_L\rho}{L}\right)\sin\left(\frac{2\pi n_L\tilde{\lambda}}{\sqrt{3}L}\right) - \sin\left(\frac{4\pi n_L\tilde{\lambda}}{\sqrt{3}L}\right)\right]$$

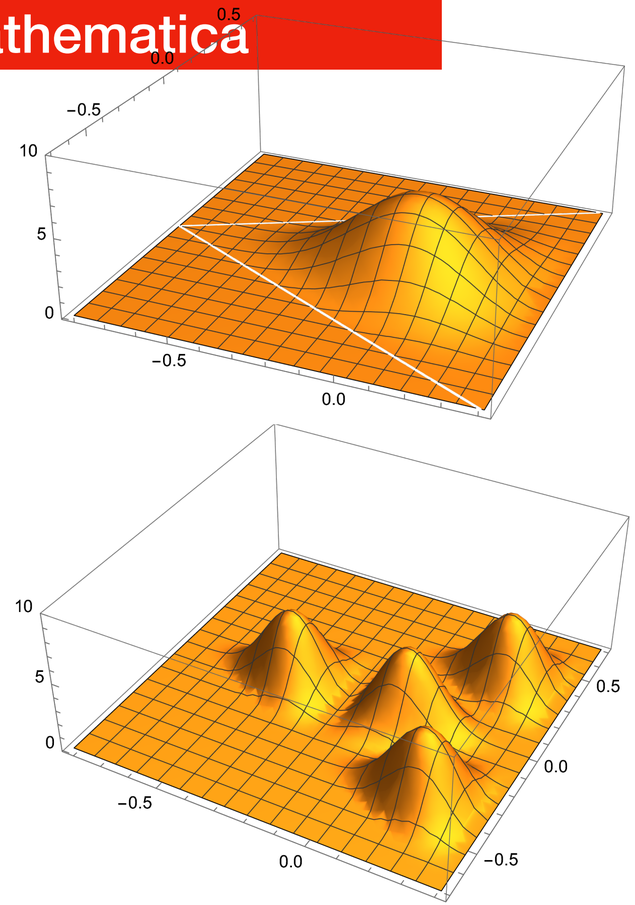

e-Print:s
2202.00167

Hadronic structure on the light-front IV. Heavy and light Baryons

$$H_{0LF} = 3(\vec{p}_\rho^{\,2} + \vec{p}_\lambda^{\,2} + 3m_Q^2)$$
$$+\frac{\sigma_T}{a}\left(|i\partial/\partial\lambda|^2 + |i\partial/\partial\rho|^2 + (3m_Q)^2(\vec{b}_\lambda^{\,2} + \vec{b}_\rho^{\,2})\right)$$

transverse oscillator plus longitudinal Laplacian

qqq, sss, ccc, bbb

The non-factorizable part of the potential is

$$\tilde{V} = \frac{\vec{p}_1^{\,2} + m_Q^2}{x_1} + \frac{\vec{p}_2^{\,2} + m_Q^2}{x_2}$$
$$+ \frac{\vec{p}_3^{\,2} + m_Q^2}{x_3} - 3(\vec{p}_1^{\,2} + \vec{p}_2^{\,2} + \vec{p}_3^{\,2}) - 9m_Q^2$$

represented by a matrix calculated in the eigenstates of H0

Single-flavor baryons

have no “good diquark” correlations
between quarks if tHooft-induced

e-Print:s
2202.00167

Hadronic structure on the light-front IV. Heavy and light Baryons

$$H_{0LF} = 3(\vec{p}_\rho^{\,2} + \vec{p}_\lambda^{\,2} + 3m_Q^2)$$
$$+\frac{\sigma_T}{a}\left(|i\partial/\partial\lambda|^2 + |i\partial/\partial\rho|^2 + (3m_Q)^2(\vec{b}_\lambda^{\,2} + \vec{b}_\rho^{\,2})\right)$$

transverse oscillator plus longitudinal Laplacian

The non-factorizable part of the potential is

$$\tilde{V} = \frac{\vec{p}_1^{\,2} + m_Q^2}{x_1} + \frac{\vec{p}_2^{\,2} + m_Q^2}{x_2} + \frac{\vec{p}_3^{\,2} + m_Q^2}{x_3} - 3(\vec{p}_1^{\,2} + \vec{p}_2^{\,2} + \vec{p}_3^{\,2}) - 9m_Q^2$$

represented by a matrix calculated in the eigenstates of H0

Single-flavor baryons

have no “good diquark” correlations between quarks if tHooft-induced

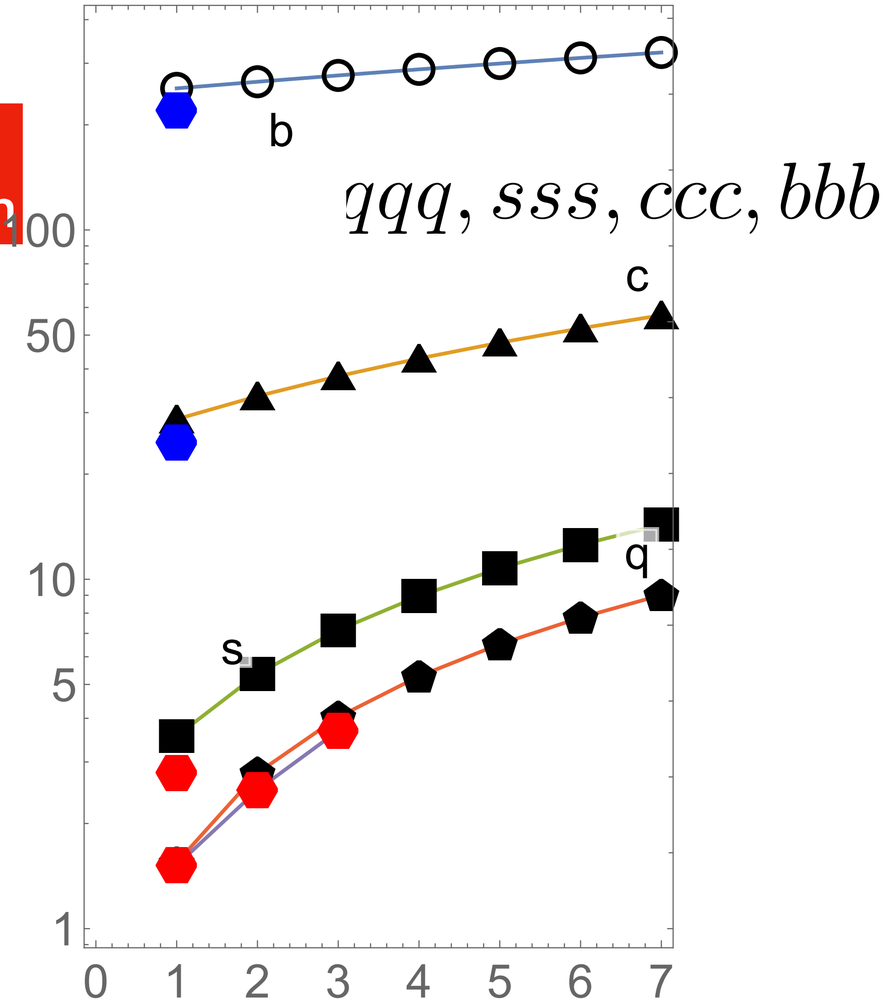

FIG. 9. Squared masses of baryons $M^2_{n+1}(Q, \frac{3}{2})$ in GeV^2, versus the principal quantum number $n+1 = 1..7$. The black circles, triangles, squared and pentagons are results of our calculations for the flavors b, c, s, q. The red hexagons are the experimental values of three Δ^{++} and one Ω^- masses, from PDG. The two blue hexagons are model predictions for masses of *ccc* and *bbb* baryons, from Table I.

e-Print:s
2202.00167

Hadronic structure on the light-front IV. Heavy and light Baryons

transverse oscillator
plus longitudinal Laplacian

$$H_{0LF} = 3(\vec{p}_\rho^{\,2} + \vec{p}_\lambda^{\,2} + 3m_Q^2)$$
$$+\frac{\sigma_T}{a}\left(|i\partial/\partial\lambda|^2 + |i\partial/\partial\rho|^2 + (3m_Q)^2(\vec{b}_\lambda^{\,2} + \vec{b}_\rho^{\,2})\right)$$

The non-factorizable part of the potential is

represented by a matrix
calculated in the eigenstates
of H0

$$\tilde{V} = \frac{\vec{p}_1^{\,2} + m_Q^2}{x_1} + \frac{\vec{p}_2^{\,2} + m_Q^2}{x_2}$$
$$+ \frac{\vec{p}_3^{\,2} + m_Q^2}{x_3} - 3(\vec{p}_1^{\,2} + \vec{p}_2^{\,2} + \vec{p}_3^{\,2}) - 9m_Q^2$$

Single-flavor baryons

have no “good diquark” correlations
between quarks if tHooft-induced

of course, we not just have all masses ,
but all light-front wave functions as well!
Can be used to calculate PDFs,FFs,GPDs

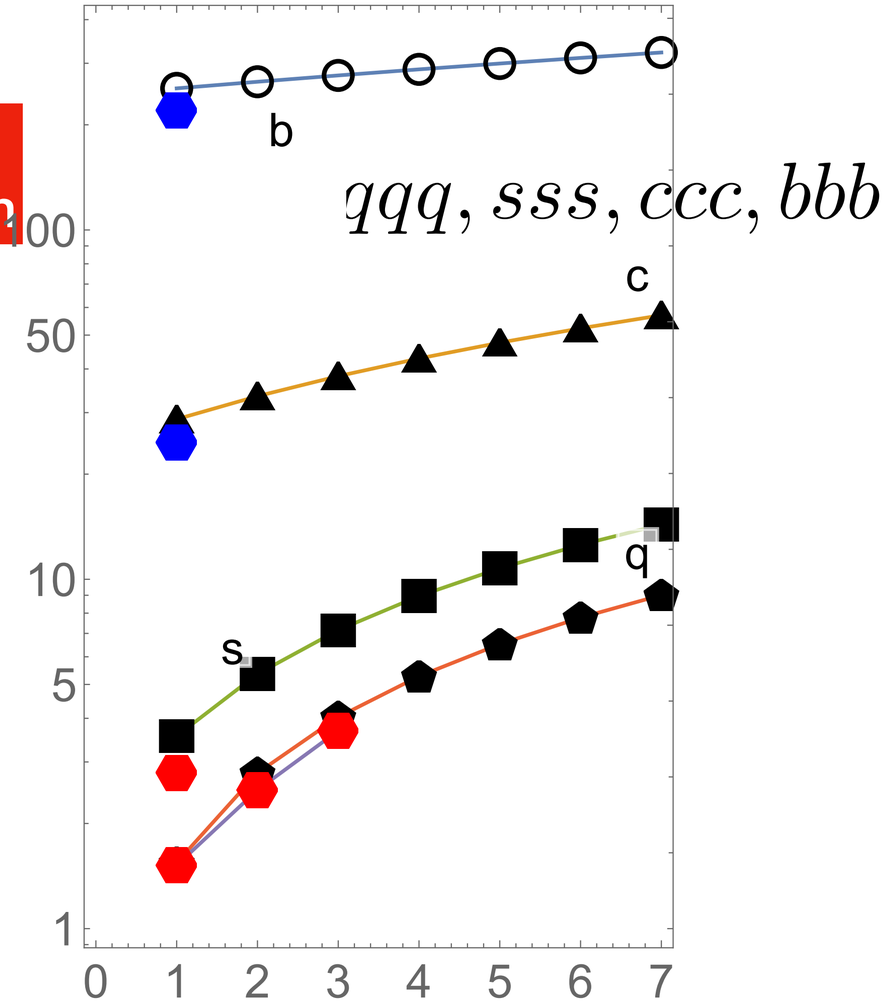

FIG. 9. Squared masses of baryons $M^2_{n+1}(Q, \frac{3}{2})$ in GeV^2, versus the principal quantum number $n+1 = 1..7$. The black circles, triangles, squared and pentagons are results of our calculations for the flavors b, c, s, q. The red hexagons are the experimental values of three Δ^{++} and one Ω^- masses, from PDG. The two blue hexagons are model predictions for masses of *ccc* and *bbb* baryons, from Table I.

red triangles are Upsilon masses
from light front Hamiltonian

same method, 12*12 matrix diagonalized
higher states affected by a cutoff

note: orbital is not L but 2d m

Squared masses for n = 0..5 (left to right)
and orbital momentum m = 0,1,2 (down to up),
calculated from the light front Hamiltonian H_{LF}

usi
u
usin

(red triangles), and shifted by a constant, $M^2 - {}_{n+1}$
5 GeV ^2^2
the blue-circles show the squared masses M^2
calculated from Schroedinger

n+1

equation in the CM frame, with only linear plus
centrifugal potentials.

**Comparison between Upsilon masses
in Schreodinger CM frame with those from light front**

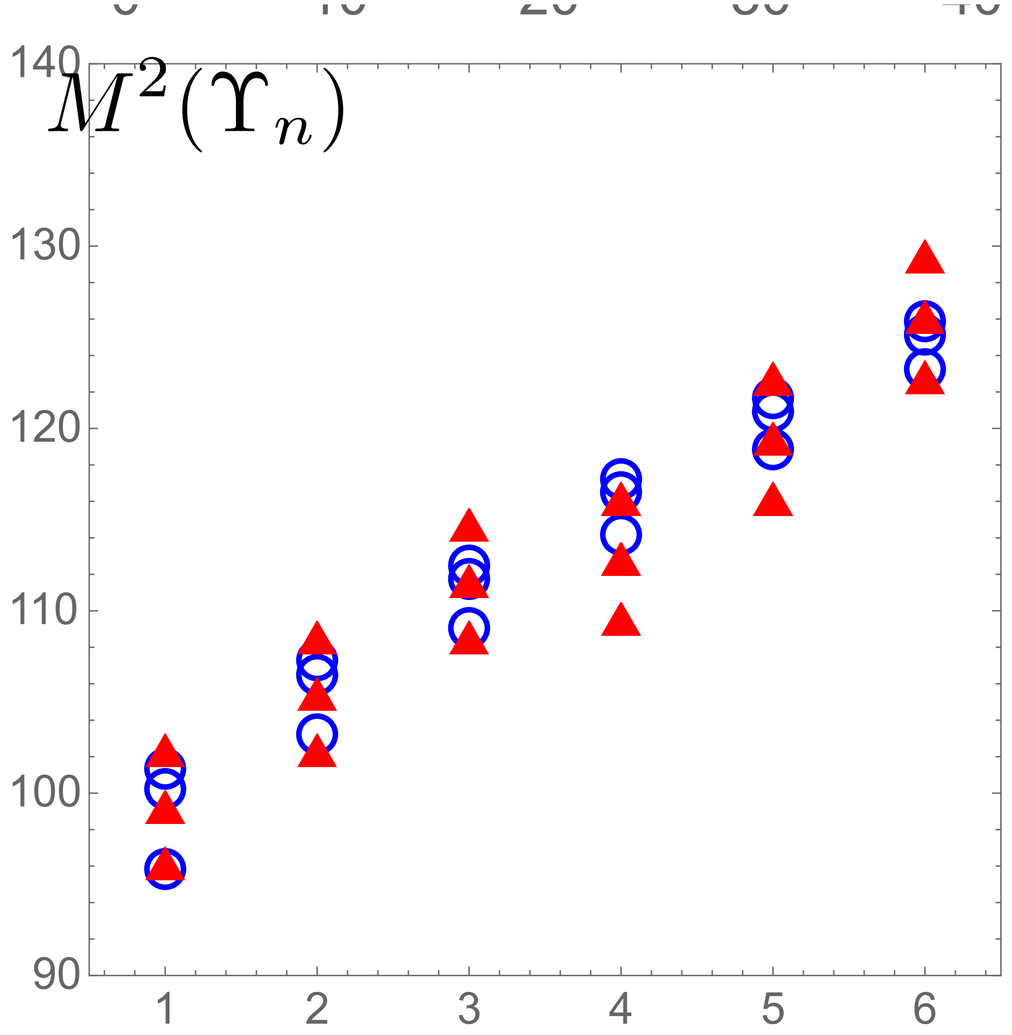

Hadronic structure on the light-front V. Diquarks, Nucleons and multiquark Fock components

e-Print: 2208.04428

phenomenology
scalar diquarks are deeply bound

assuming that the standard spin-spin interactions are of the form $(\vec{\sigma 1}\vec{\sigma 2})$,

this spin interaction can be eliminated

$$M(1{+}ud) - M(0{+}ud)\ (1) \approx$$

$$(2M(\Sigma^{*}Q) + M(\Sigma Q)/3 - M(\Lambda Q) \approx 0.21\ \text{GeV}$$

the instanton-induced 't Hooft vertex.

$$\frac{G_{qq}}{G_{\bar{q}q}} = \frac{1}{N_c - 1}$$

so it is 1 for Nc=2 and 1/2 for Nc=3 and -1 in QED

Hadronic structure on the light-front V. Diquarks, Nucleons and multiquark Fock components

e-Print: 2208.04428

phenomenology
scalar diquarks are deeply bound

diquarks are baryons in Nc=2 theory
which has Pauli-Gursey symmetry
so scalar diquark is degenerate with the pion
and vector degenerate with vector mesons

the instanton-induced ’t Hooft vertex.

$$\frac{G_{qq}}{G_{\bar{q}q}} = \frac{1}{N_c - 1}$$

so it is 1 for Nc=2
and 1/2 for Nc=3
and -1 in QED

assuming that the standard spin-spin interactions are of the form $(\vec{\sigma 1}\vec{\sigma 2})$,

this spin interaction can be eliminated

$$M(1{+}ud) - M(0{+}ud)\ (1) \approx$$

$$(2M(\Sigma^* Q) + M(\Sigma Q)/3 - M(\Lambda Q) \approx 0.21\ \mathrm{GeV}$$

Hadronic structure on the light-front V. Diquarks, Nucleons and multiquark Fock components

e-Print: 2208.04428

phenomenology
scalar diquarks are deeply bound

diquarks are baryons in Nc=2 theory
which has Pauli-Gursey symmetry
so scalar diquark is degenerate with the pion
and vector degenerate with vector mesons

the instanton-induced ’t Hooft vertex.

$$\frac{G_{qq}}{G_{\bar{q}q}} = \frac{1}{N_c - 1}$$

so it is 1 for Nc=2
and 1/2 for Nc=3
and -1 in QED

assuming that the standard spin-spin interactions are of the form $(\vec{\sigma 1}\vec{\sigma 2})$,

this spin interaction can be eliminated

$$M(1{+}ud) - M(0{+}ud)\ (1) \approx$$

$$(2M(\Sigma^* Q) + M(\Sigma Q)/3 - M(\Lambda Q) \approx 0.21\ \text{GeV}$$

Scalar diquarks become
Cooper pair in dense quark matter
=> color superconductors

Hadronic structure on the light-front V. Diquarks, Nucleons and multiquark Fock components

e-Print: 2208.04428

phenomenology
scalar diquarks are deeply bound

assuming that the standard spin-spin interactions are of the form $(\vec{\sigma 1}\vec{\sigma 2})$,

this spin interaction can be eliminated

$$M(1{+}ud) - M(0{+}ud)\ (1) \approx$$
$$(2M(\Sigma^{*}Q) + M(\Sigma Q)/3 - M(\Lambda Q) \approx 0.21\ \text{GeV}$$

diquarks are baryons in Nc=2 theory
which has Pauli-Gursey symmetry
so scalar diquark is degenerate with the pion
and vector degenerate with vector mesons

the instanton-induced 't Hooft vertex.

$$\frac{G_{qq}}{G_{\bar{q}q}} = \frac{1}{N_c - 1}$$

so it is 1 for Nc=2
and 1/2 for Nc=3
and -1 in QED

Scalar diquarks become
Cooper pair in dense quark matter
=> color superconductors

Diquark Bose condensates in high density matter and instantons
R.Rapp, Thomas Schäfer, Edward V. Shuryak, M. Velkovsky
Phys.Rev.Lett. 81 (1998) 53-56 • e-Print: hep-ph/9711396

DIQUARK PAIRING IN THE NUCLEONS

quasilocal approximation N versus Delta masses and WFs

$$H_{ud} = -G_{ud}\delta(\vec{r}_u - \vec{r}_d)$$

two diquark correlation channels in N (d with 2 u's) already makes noticeable differencesfor WFs especially near x->1

note that effect of pairing is smaller in excited states

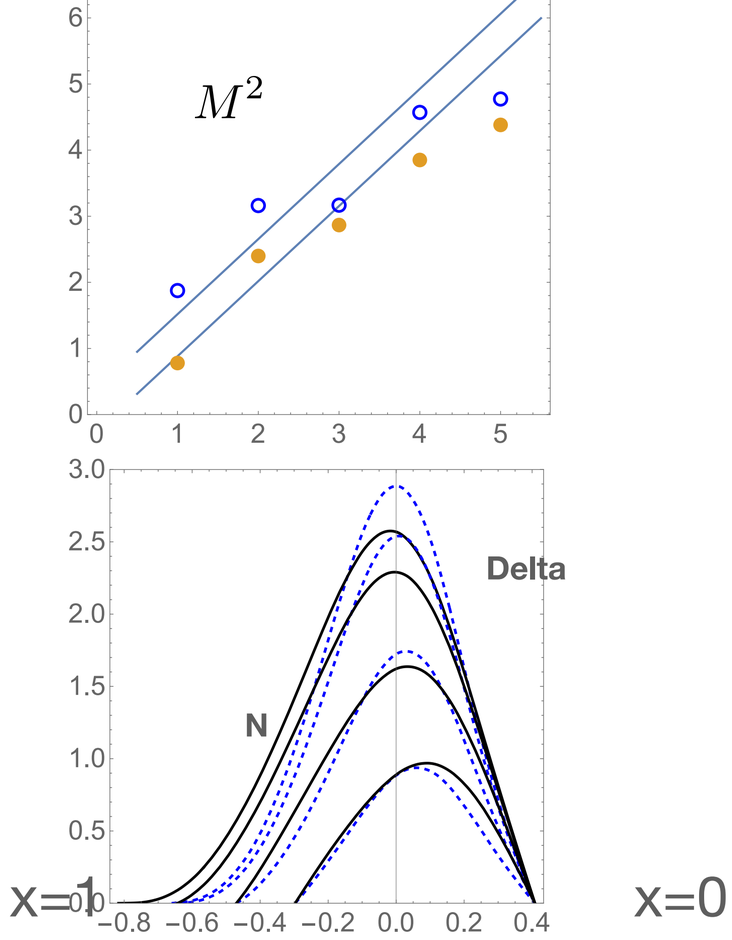

FIG. 6: Upper: Squared masses of the Delta (open points) and N (closed) resonances versus their successive quantum number n. The two straight lines shown for comparison, are the Regge trajectories fitted to the experimental values of $M^2(J)$, versus the total angular momentum J, with the slope $\alpha' = 0.88\,GeV^2$.
Lower: LFWFs for the lowest Delta (dashed lines) and N (solid lines). The plots are shown versus the Jacobi coordinate λ, for fixed $\rho = 0, 0.1, 0.2, 0.3$, top to bottom.

e-Print: 2208.04428

Nucleon and Delta Formfactors are approximately 1/Q^4

but show differences at large enough Q, Delta is softer which means its size is about 2^(1/4) times larger

$$F_1(t) = \int dx H(x,0,t) \qquad \textbf{N}$$

$$A(t) = \int dx\, x H(x,0,t)$$

$$A(Q^2)/F_1(Q^2) \qquad \textbf{Delta}$$

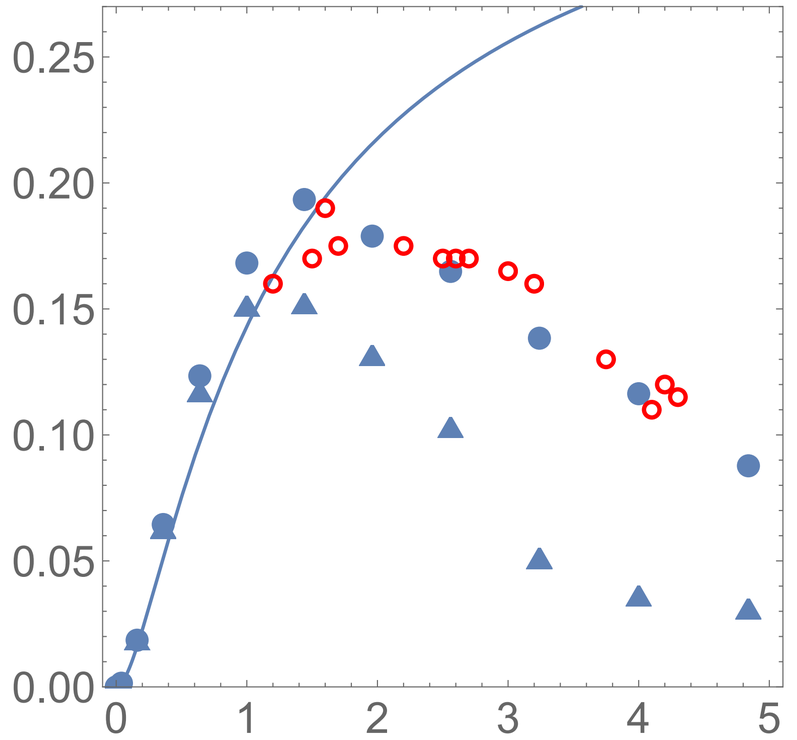

N

Delta

FIG. 8: $Q^4 F_1^d(Q^2)$, (GeV^4) versus the momentum transfer Q^2 (GeV^2). The triangles and closed points correspond to the Delta and Proton LFWFs, respectively. The red circles are extraction from the experimental data on the p and n formfactors mentioned in the text. The solid line shown for comparison, corresponds to the dipole form factor $Q^4/(1+Q^2/m_\rho^2)^2$.

Nucleon and Delta Formfactors are approximately 1/Q^4

but show differences at large enough Q, Delta is softer which means its size is about 2^(1/4) times larger

gravitational formfactors from GPDs

$$F_1(t) = \int dx H(x,0,t) \qquad \textbf{N}$$

$$A(t) = \int dx\, x H(x,0,t)$$

$A(Q^2)/F_1(Q^2)$ **Delta**

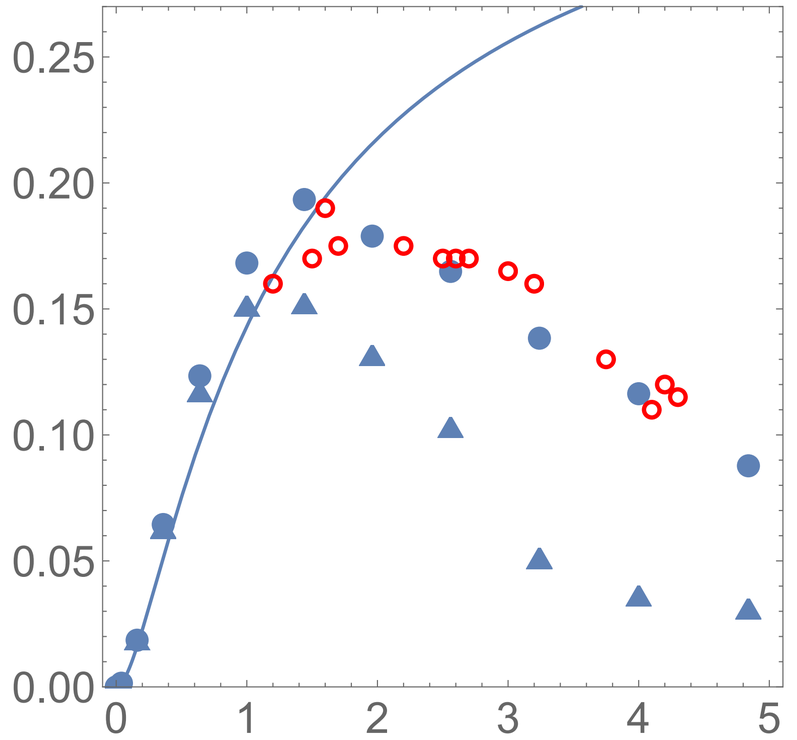

N

Delta

FIG. 8: $Q^4 F_1^d(Q^2)$, (GeV^4) versus the momentum transfer Q^2 (GeV^2). The triangles and closed points correspond to the Delta and Proton LFWFs, respectively. The red circles are extraction from the experimental data on the p and n formfactors mentioned in the text. The solid line shown for comparison, corresponds to the dipole form factor $Q^4/(1+Q^2/m_\rho^2)^2$.

Nucleon and Delta Formfactors are approximately 1/Q^4

but show differences at large enough Q, Delta is softer which means its size is about 2^(1/4) times larger

gravitational formfactors from GPDs

$$F_1(t) = \int dx H(x,0,t)$$

$$A(t) = \int dx\, x H(x,0,t)$$

$A(Q^2)/F_1(Q^2)$

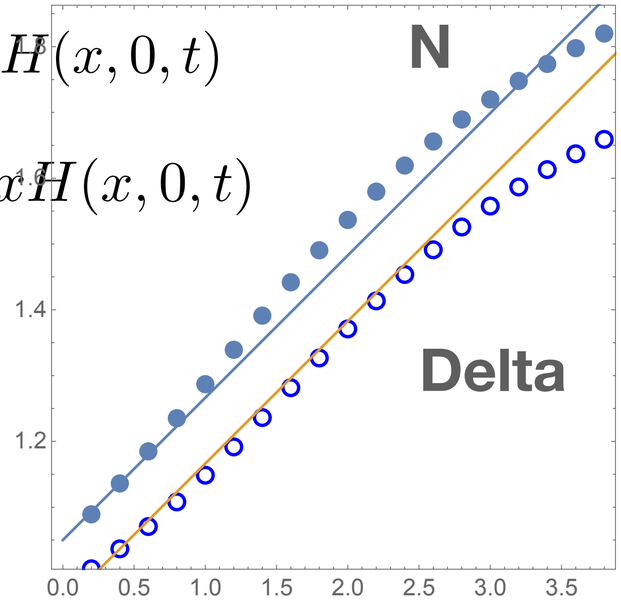

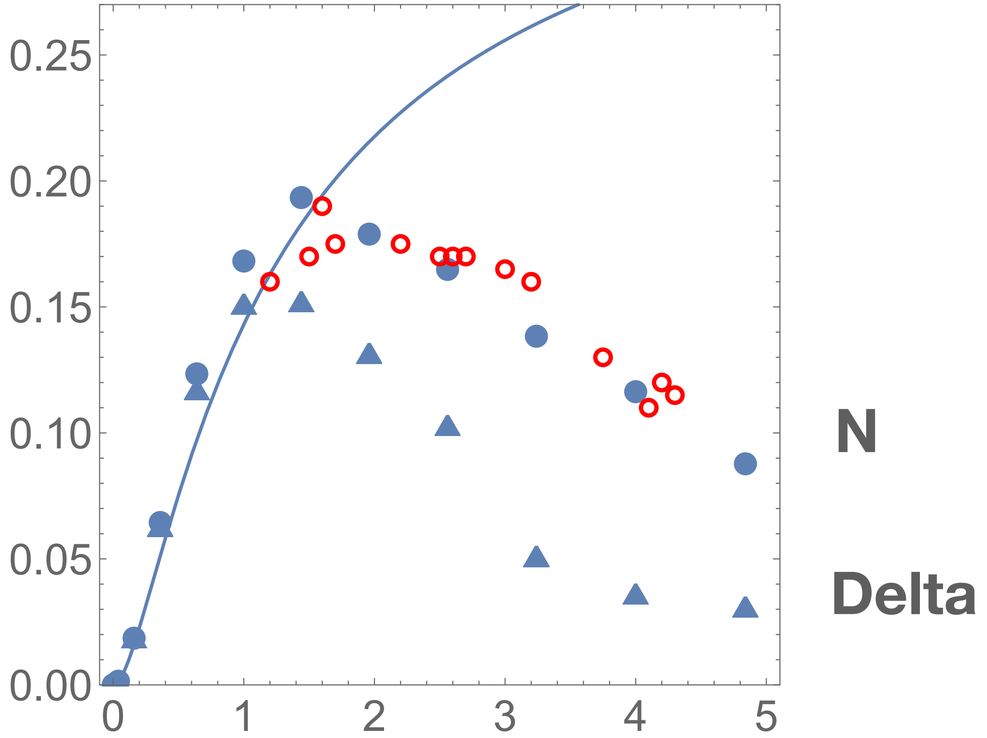

FIG. 8: $Q^4 F_1^d(Q^2)$, (GeV^4) versus the momentum transfer Q^2 (GeV^2). The triangles and closed points correspond to the Delta and Proton LFWFs, respectively. The red circles are extraction from the experimental data on the p and n formfactors mentioned in the text. The solid line shown for comparison, corresponds to the dipole form factor $Q^4/(1+Q^2/m_\rho^2)^2$.

paper VI

Nucleon and Delta GPDs

e-Print: 2301.12238

Zero skewness:

$$H(x,0,t) = \int_P \delta(x-x_1)\,\psi^{+*}([x_i', k_{i\perp}', \lambda_i])\psi^{+}([x_i, k_{i\perp}, \lambda_i])$$

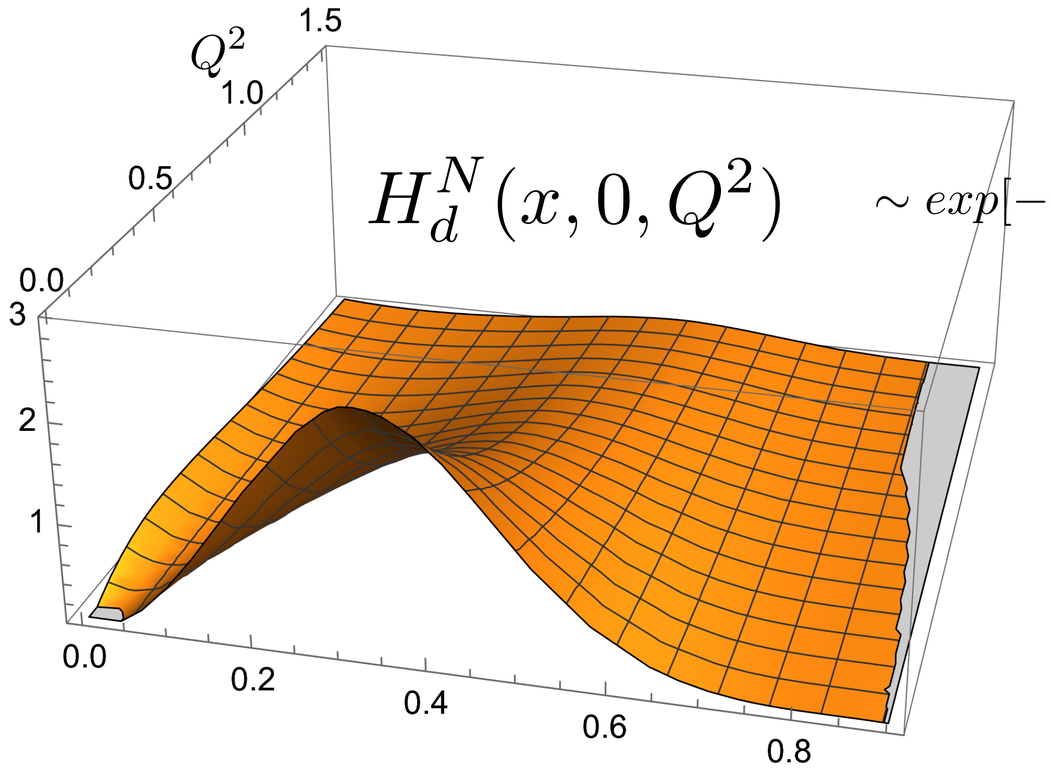

$$H_d^N(x,0,Q^2) \quad \sim exp[-Q^2 R^2(x)/2]$$

$$-\partial log[H]/\partial Q^2$$

N

Δ

paper VI

Nucleon and Delta GPDs

e-Print: 2301.12238

Zero skewness:

$$H(x,0,t) = \int_P \delta(x-x_1)\,\psi^{+*}([x_i', k_{i\perp}', \lambda_i])\psi^{+}([x_i, k_{i\perp}, \lambda_i])$$

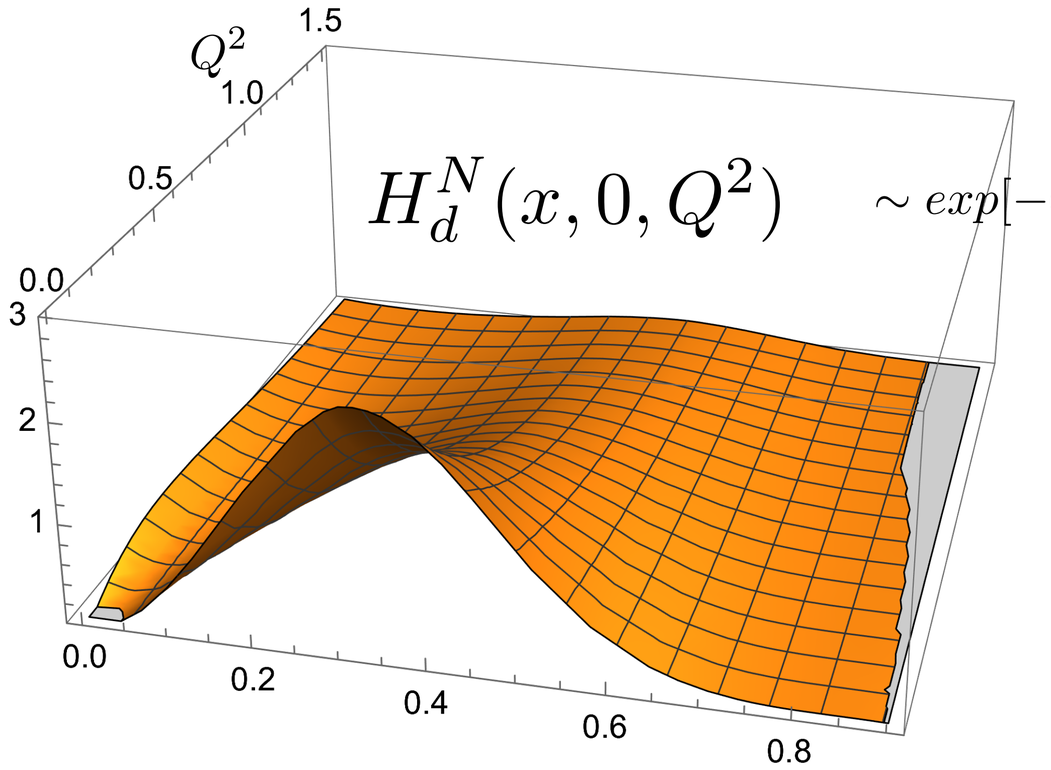

$$H_d^N(x,0,Q^2) \quad \sim exp[-Q^2 R^2(x)/2]$$

it is a formfactor
but for particular
x of the struck quark,
and that turns out to be
Gaussians, with
x-dependent slopes

$$-\partial log[H]/\partial Q^2$$

N

Δ

paper VI

Nucleon and Delta GPDs

e-Print: 2301.12238

Zero skewness:

$$H(x,0,t) = \int_P \delta(x-x_1)\,\psi^{+*}([x_i', k_{i\perp}', \lambda_i])\psi^{+}([x_i, k_{i\perp}, \lambda_i])$$

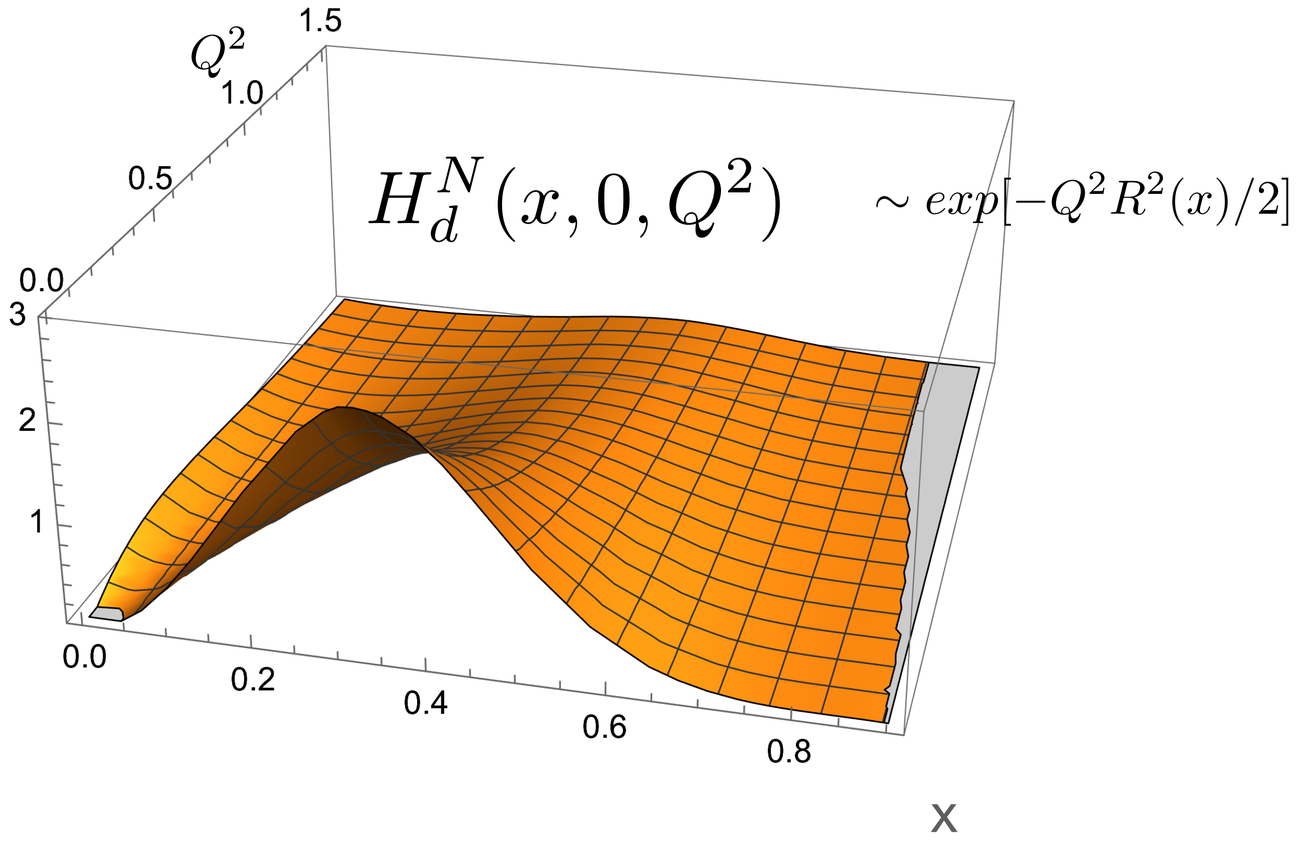

it is a formfactor
but for particular
x of the struck quark,
and that turns out to be
Gaussians, with
x-dependent slopes

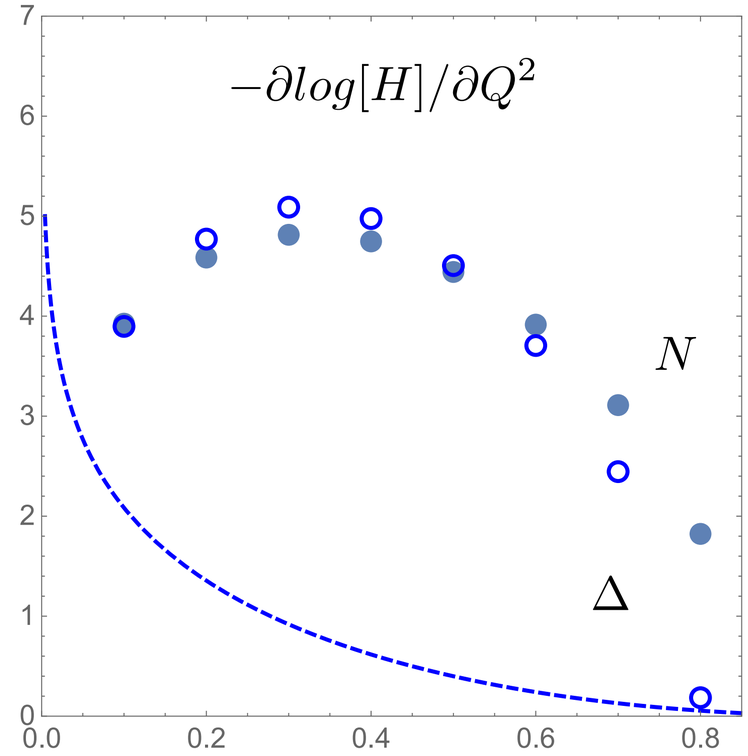

paper VI # Nucleon and Delta GPDs

e-Print: 2301.12238

Zero skewness:

$$H(x,0,t) = \int_P \delta(x-x_1)\,\psi^{+*}([x_i', k_{i\perp}', \lambda_i])\psi^{+}([x_i, k_{i\perp}, \lambda_i])$$

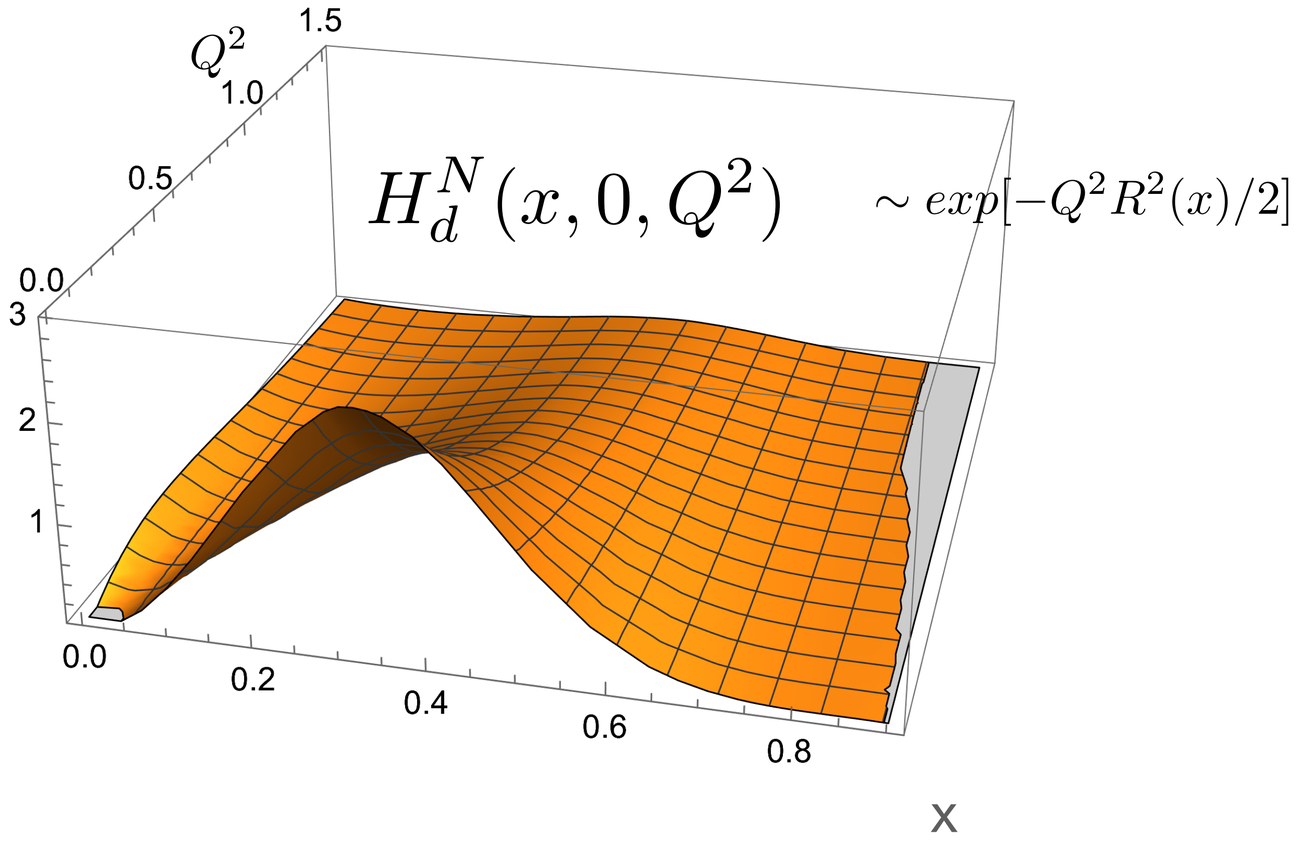

it is a formfactor
but for particular
x of the struck quark,
and that turns out to be
Gaussians, with
x-dependent slopes

so ff\sim 1/Q^4
appears only
after x integration

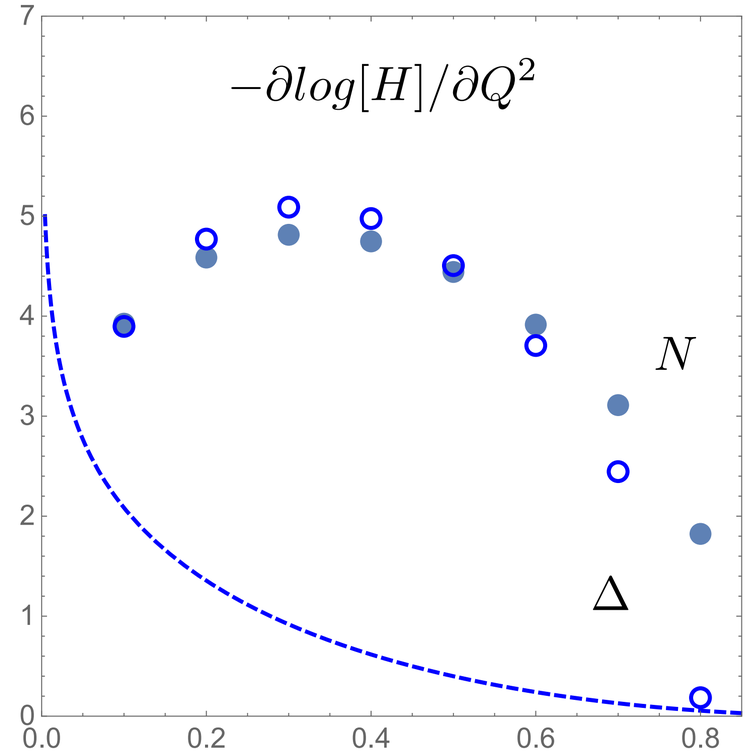

Compairing GPDs,
our calculations (dashed)
with lattice results
(solid)

one finds agreement
at x>0.4 or so
as one should expect

small x includes antiquarks
and gluons
(mu=2 GeV^2)
which we do not include

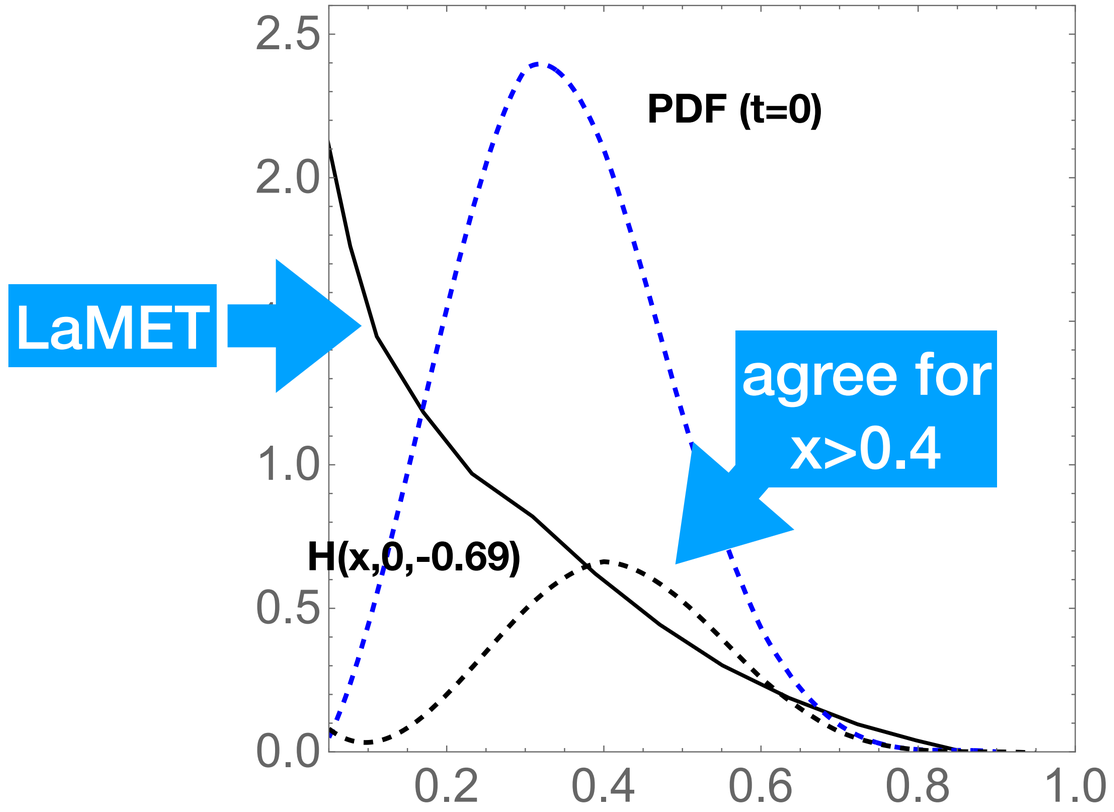

FIG. 6: We show the lattice baryonic GPD $H(x, \xi = 0, t = -0.69\,\mathrm{GeV}^2)$ versus $x$following from LaMET in [18] (black-solid line), and our result (dashed-black line). Our result for the GPD $H(x, \xi = 0, t = 0)$ which is the PDF (dashed-blue line), is shown for comparison.

Revolution in hadronic spectroscopy -> multiquark hadrons

since 1960's they were considered "exotics" with questionable experimental support, but not anymore

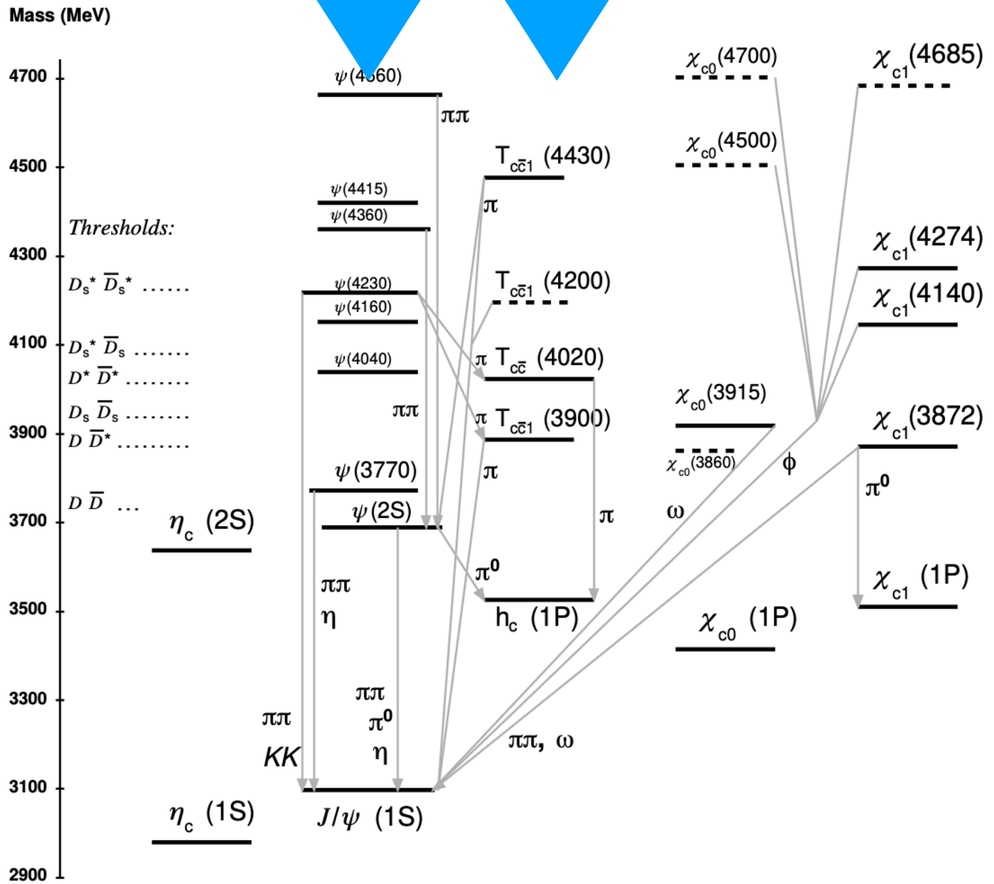

in axial 1^+- channel **4 tetras** and only one charmonium
in vector 1^— 9 psi's out of which only 5 charmonia
and also **4 tetras**

χ_{c2} (3930)

ψ_2(3823)

ψ_3 (3842)

χ_{c2} (1P)

Tells us about adding quark pair as sigma and pion

All-charm tetraquarks data

first observed by the LHCb Collaboration, and subsequently by the CMS and ATLAS, in J/ψ J/ψ (and related) decay channels. Three interfering states have been reported, all with the same quantum numbers, most likely 2++.

$$M_1 = 6593^{+15}_{-14}, \qquad \Gamma_1 = 446^{+66}_{-54},$$
$$M_2 = 6847 \pm 10, \qquad \Gamma_2 = 135^{+16}_{-14},$$
$$M_3 = 7173^{+9}_{-10}, \qquad \Gamma_3 = 73^{+18}_{-15},$$

Tetraquarks kinematics and color dynamics

2308.05638

(like for 4He in original NP applications)

$$\boldsymbol{\xi}_1 = \sqrt{\frac{1}{2}}(\mathbf{r}_1 - \mathbf{r}_2)$$

$$\boldsymbol{\xi}_2 = \sqrt{\frac{1}{6}}(\mathbf{r}_1 + \mathbf{r}_2 - 2\mathbf{r}_3)$$

$$\boldsymbol{\xi}_3 = \frac{1}{2\sqrt{3}}(\mathbf{r}_1 + \mathbf{r}_2 + \mathbf{r}_3 - 3\mathbf{r}_4)$$

$$-2mK = \frac{\partial^2}{\partial \boldsymbol{\xi}_1^2} + \frac{\partial^2}{\partial \boldsymbol{\xi}_2^2} + \frac{\partial^2}{\partial \boldsymbol{\xi}_3^2} + \frac{1}{4}\frac{\partial^2}{\partial \mathbf{X}^2}$$

Kinetic energy

$$R_9^2 \equiv \boldsymbol{\xi}_1^2 + \boldsymbol{\xi}_2^2 + \boldsymbol{\xi}_3^2$$
$$= \frac{1}{4}[(\mathbf{r}_1 - \mathbf{r}_2)^2 + (\mathbf{r}_1 - \mathbf{r}_3)^2 + (\mathbf{r}_1 - \mathbf{r}_4)^2$$
$$+ (\mathbf{r}_3 - \mathbf{r}_2)^2 + (\mathbf{r}_4 - \mathbf{r}_2)^2 + (\mathbf{r}_3 - \mathbf{r}_4)^2]$$

Jacobi coordinates

hyperdistance

$$H_{\lambda\lambda} = \sum_{i>j} w_{ij}(\boldsymbol{\lambda}_i \boldsymbol{\lambda}_j),$$

$$H^{66}_{\lambda\lambda} = \frac{2}{3}\,(2w_{12} - 5w_{13} - 5w_{14} - 5w_{24} - 5w_{32} + 2w_{34}),$$

$$H^{\underline{33}}_{\lambda\lambda} = -\frac{4}{3}\,(2w_{12} + w_{13} + w_{14} + w_{24} + w_{32} + 2w_{34}).$$

In the 66 case, the contributions from qq and $\bar{q}\bar{q}$ pairs are repulsive, whereas in the $\underline{33}$ case all terms are attractive. A naive application of the diquark model would therefore suggest that the $\underline{33}$ configuration should have a lower energy than the 66 one. However, this conclusion is incorrect. If all interaction strengths are equal, $w_{ij} = w$, both expressions reduce to the same value, $-(32w/3)$.

$$\psi(R_9) = u(R_9)/R_9^4$$

$$\mathrm{H}=\left[\ \left(-\frac{d^2}{dR_9^2}+\frac{12}{R_9^2}\right)\frac{1}{2M}+(4M+V)\ \right]\mathrm{u}$$

2308.05638

$$M(2S) - M(1S) \approx 370\,MeV$$

$$M(3S) - M(1S) \approx 689\,MeV$$

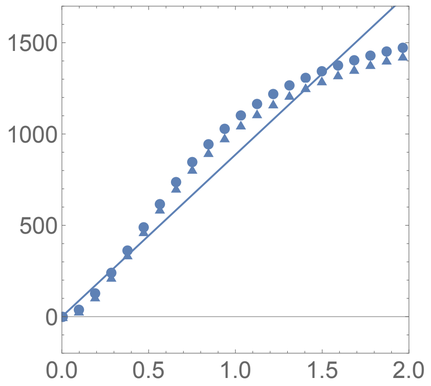

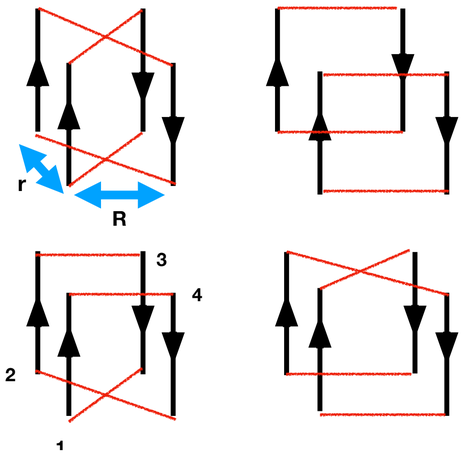

experiment (ATLAS)

$$M(2) - M(1) \approx 250\,MeV$$

$$M(3) - M(1) \approx 600\,MeV$$

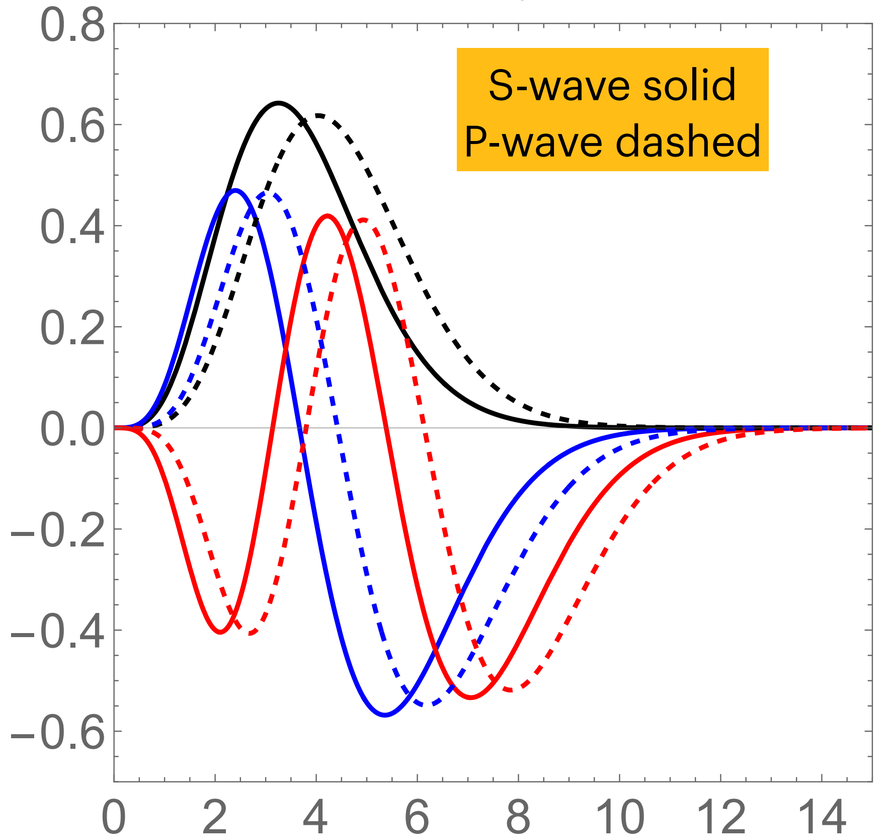

Novel technique to find multiquark states which obey Fermi statistics (started from P-shell and D-shell baryons)

[Miesch and Shuryak, 2024].

S-shell (L = 0) pentaquarks has color-spin-flavor dimension of ``monom'' space $36 \times 25 \times 25 = 746496$,

P-shell (L = 1) states. another factor of 4, in total O(10^6) monoms

:

At first sight, writing operators as matrices in such a large space may appear prohibitive, even with the aid of Mathematica. Fortunately, this is not the case, And how to enforce Fermi statistics?

We worked out representations of permutation groups S(n)
Procedure:
(1) find 2 generators of S_n group as explicit matrices,
(2)diagonalize those,
(3) find common eigenvectors of them with eigenvalues -1

Hexaquarks, q^6, as example of multiquark state

For maximal spin S=3 the antisymmetric color-isospin wave function was derived by [Kim et al., 2020].

explicit expression as a sum of five terms with different color-flavor structures

It is perhaps the state observed as the resonance d(2380) in the reaction $p + n \to d + \pi^0 + \pi^0$.

Its width, $\Gamma_{d^*} \approx 70\,\mathrm{MeV}$, is significantly smaller than that of the Δ baryon, $\Gamma_\Delta \approx 115\,\mathrm{MeV}$, which was one of the arguments against interpreting it as a loosely bound $\Delta\Delta$ state. Moreover, a deuteron-like $\Delta\Delta$ interpretation would require a binding energy of order $\approx 84\,\mathrm{MeV}$, which appears uncomfortably large.

we reproduce this one
and derived wave functions for all values of spin

[Miesch and Shuryak, 2024].

Why are pentaquarks important?
they admix to baryons...

Geiger and Isgur, 1990

an extra $q^{-}q$ pair with σ
(vacuum)
quantum numbers

in a $^3P_0$ state
(J = 0, S = 1, L = 1)

others added a pair
as a pion
also include momentum

Pentaquarks on the ligh front...
e-Print: 2510.23404

Why are pentaquarks important? they admix to baryons...

Geiger and Isgur, 1990

an extra $q^{-}q$ pair with σ (vacuum) quantum numbers

in a $^3P_0$ state ($J = 0, S = 1, L = 1$)

others added a pair as a pion also include momentum

Pentaquarks on the ligh front...
e-Print: 2510.23404

we solved those in CM and LF
P-wave pentaquarks are 27
not easy but doable

admixture is not small!
explains spin puzzle and antiquark flavor anysotropy

Spin-isospin table of antisymmetric S-shell (L = 0) pentaquark
The integers denote state multiplicities, while the numbers in parentheses give the dimensions of the corresponding good basis.

S-shell

I/S	1/2	3/2	5/2
1/2	3 (75)	3 (60)	1 (15)
3/2	3 (60)	3 (48)	1 (12)
5/2	1 (15)	1 (12)	0

$$N_{GB} = N_{GB}^{\text{color}} \times N_{GB}^{\text{spin}} \times N_{GB}^{\text{flavor}}.$$

$$H_{\lambda\sigma} = -C_{\lambda\sigma} \sum_{i>j} (\boldsymbol{\lambda}_i \boldsymbol{\lambda}_j)(\mathbf{S}_i \mathbf{S}_j).$$

S	1/2	1/2	1/2	3/2	3/2	3/2	5/2
$\lambda\lambda$	-40/3	-40/3	-40/3	-40/3	-40/3	-40/3	-40/3
SS	-3/2	-3/2	-3/2	0	0	0	5/2
$H_{\lambda\sigma}/C_{\lambda\sigma}$	-4.66	-1.44	2.77	-3	1/3	10/3	10/3

Pentaquarks
e-Print: 2507.01861
on the light front...
e-Print: 2510.23404

P-shell

I/S	1/2	3/2	5/2
1/2	13 (300)	11 (240)	3 (60)
3/2	11 (240)	10 (192)	3 (48)
5/2	3 (60)	3 (48)	1 (12)

Where pentaquarks become chaotic?

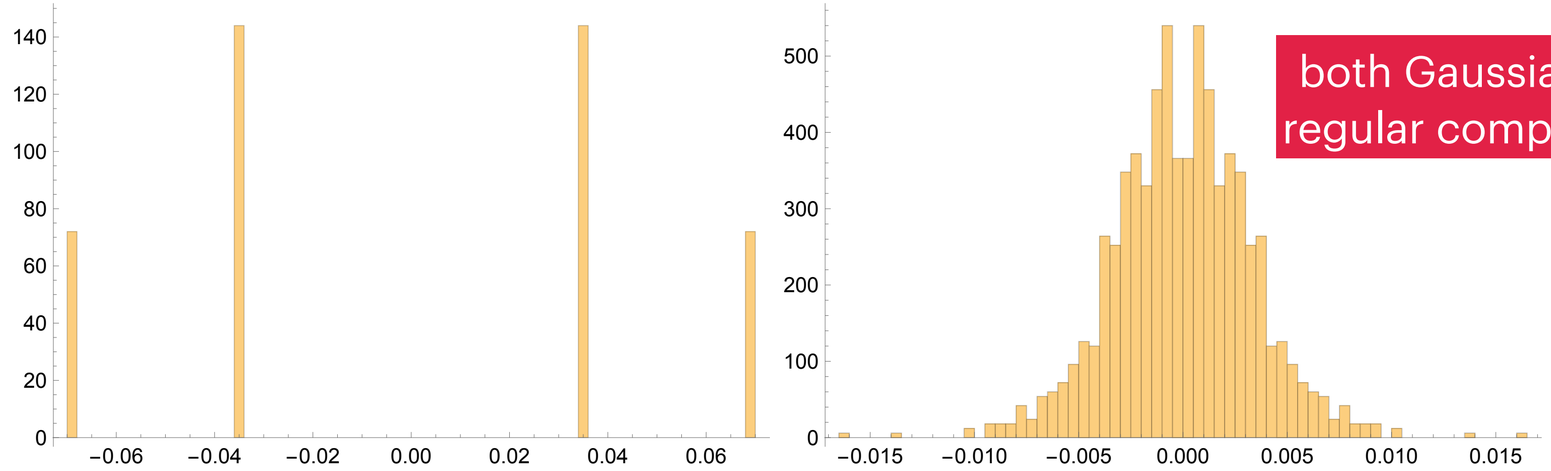

Fig. 9.3.2 Distribution of monom coefficients for an S-shell state with $L = 0$, $S = 5/2$, $I = 1/2$ (upper panel) and for a P-shell state with $L = 1$, $S = 1/2$, $I = 1/2$ (lower panel).

Quantum few-body systems are known to undergo a transition to the so-called quantum chaos regime

This phenomenon is well documented in atomic and nuclear systems with several particles or holes near closed shells. A historically important example is the cerium atom, which has four valence electrons and thus 12 effective coordinates.
even its lowest-energy states display chaotic behavior

Pentaquarks on the LF

I/S_z	1/2	3/2	5/2
-5/2	1 (15)	1 (12)	0
-3/2	4 (75)	4 (60)	1 (15)
-1/2	7 (150)	7 (120)	2 (30)
1/2	7 (150)	7 (120)	2 (30)
3/2	4 (75)	4 (60)	1 (15)
5/2	1 (15)	1 (12)	0

S-shell

I/S_z	1/2	3/2	5/2
-5/2	3 (60)	3 (48)	1 (12)
-3/2	14 (300)	13 (240)	4 (60)
-1/2	27 (600)	24 (480)	7 (120)
1/2	27 (600)	24 (480)	7 (120)
3/2	14 (300)	13 (240)	4 (60)
5/2	3 (60)	3 (48)	1 (12)

P-shell

$$
\begin{aligned}
x_1 &= (6 + 15\sqrt{2}\alpha + 5\sqrt{6}\beta + 5\sqrt{3}\gamma + 3\sqrt{5}\delta)/30 \\
x_2 &= (6 - 15\sqrt{2}\alpha + 5\sqrt{6}\beta + 5\sqrt{3}\gamma + 3\sqrt{5}\delta)/30, \\
x_3 &= (6 - 10\sqrt{6}\beta + 5\sqrt{3}\gamma + 3\sqrt{5}\delta)/30, \\
x_4 &= 1/10(2 - 5\sqrt{3}\gamma + \sqrt{5}\delta), \\
x_5 &= 1/5 - (2\delta)/\sqrt{5} \qquad (
\end{aligned}
$$

A4 simplex or "starfish" on which LFWF is calculated similar to triangle

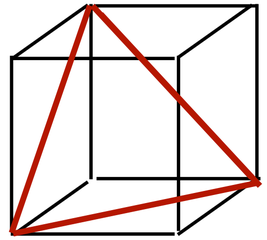

P-shell pentas admixed to the proton

operator	$p\sigma$	$N\pi$	$\Delta\pi$
$S_z(5)$	-0.177	-0.112	-0.0338
$\bar{d} = I_+(5)$	0.81	0.858	0.333
$\bar{u} = I_-(5)$	0.19	0.142	0.666

TABLE III. Some properties of the three 5-quark admix
tures to the nucleon (24) defined as average values of th
operators listed in the first column.

Pentaquarks on the LF

I/S_z	1/2	3/2	5/2
-5/2	1 (15)	1 (12)	0
-3/2	4 (75)	4 (60)	1 (15)
-1/2	7 (150)	7 (120)	2 (30)
1/2	7 (150)	7 (120)	2 (30)
3/2	4 (75)	4 (60)	1 (15)
5/2	1 (15)	1 (12)	0

S-shell

I/S_z	1/2	3/2	5/2
-5/2	3 (60)	3 (48)	1 (12)
-3/2	14 (300)	13 (240)	4 (60)
-1/2	27 (600)	24 (480)	7 (120)
1/2	27 (600)	24 (480)	7 (120)
3/2	14 (300)	13 (240)	4 (60)
5/2	3 (60)	3 (48)	1 (12)

P-shell

P-shell pentas admixed to the proton

operator	$p\sigma$	$N\pi$	$\Delta\pi$
$S_z(5)$	-0.177	-0.112	-0.0338
$\bar{d} = I_+(5)$	0.81	0.858	0.333
$\bar{u} = I_-(5)$	0.19	0.142	0.666

TABLE III. Some properties of the three 5-quark admix tures to the nucleon (24) defined as average values of th operators listed in the first column.

$$
\begin{aligned}
x_1 &= (6 + 15\sqrt{2}\alpha + 5\sqrt{6}\beta + 5\sqrt{3}\gamma + 3\sqrt{5}\delta)/30 \\
x_2 &= (6 - 15\sqrt{2}\alpha + 5\sqrt{6}\beta + 5\sqrt{3}\gamma + 3\sqrt{5}\delta)/30, \\
x_3 &= (6 - 10\sqrt{6}\beta + 5\sqrt{3}\gamma + 3\sqrt{5}\delta)/30, \\
x_4 &= 1/10(2 - 5\sqrt{3}\gamma + \sqrt{5}\delta), \\
x_5 &= 1/5 - (2\delta)/\sqrt{5} \qquad (
\end{aligned}
$$

A4 simplex or "starfish" on which LFWF is calculated similar to triangle

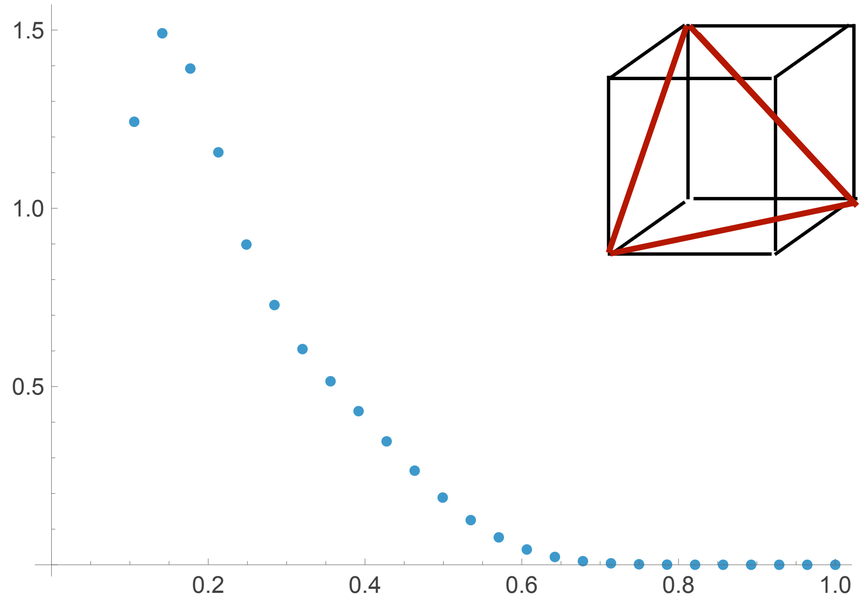

FIG. 9. Predicted PDF of the antiquarks, from $\Delta\psi_{p\sigma}$ (arbitrary units) versus Bjorken momentum fraction x. This plot is linear, emphasising the small x region.

Summary of lecture 1

1. **Jacobi coordinates used, both in CM and LF spectroscopy: no fake variables**
2. **LF mesons, baryons ... pentaquarks quantized in momentum representation**
3. **all defined on proper manifolds**
4. **basic model: constituent quark+confinement, in N diquark correlations**
5. **Novel methods to enforce Fermi statistics, used for 5,6 and more light quarks**
6. **spin problem + antiquark PDFs from pentaquark admixture to nucleons**

Preview of lecture 2

1. Topological landscape, sphalerons and instantons
2. Instanon-based forces, 't Hooft Lagrangian
3. Instanton liquid model
4. Chiral symmetry breaking
5. instanton-antiinstanton molecules
6. generation of interquark potentials
7. spin-dependent forces

extra slides

Bridging the gap between hadronic spectroscopy and partonic physics

$$\mu^2 \approx 1\,GeV^2$$

The *first ark of the bridge* (described in detail in these series of works) is to transfer such quark models from the CM frame to the light front. For some simplest cases – like heavy quarkonia – it amounts to a transition from spherical to cylindrical coordinates, with subsequent transformation of longitudinal momenta into Bjorken-Feynman variable x. But in general, it is easier to start with light-front Hamiltonians H_{LF} and perform its quantization. One of the benefit is that no nonrelativistic approximation is needed, therefore heavy and light quarks are treated in the same way.

The *second ark of the bridge* is built via *chiral dynamics* , which seeds the quark sea by producing extra quark-antiquark pair. In section VIII we discuss how it can be done, in the first order in 't Hooft effective action as well as via intermediate pions.

$$1\,Gev^2 < \mu^2 < 2\,GeV^2$$

We will then argue that as the *third ark of the bridge* one should use the well known DGLAP evolution of the PDFs (perhaps modified), down to the scale at which there are no gluons. There the $q\bar{q}$ sea should be reduced to only the part generated by chiral dynamics (step two). The antiquark flavor asymmetry $\bar{d}-\bar{u}$ is the tool allowing us to tell gluon and chiral contributions, as it cannot be generated by "flavor blind" gluons.

Gaps between levels
gapn = Mn+1 −M1 versus n.
Blue disks, orange disks, and green triangles
correspond to s¯s, c¯c, and b¯b quarkonia
(ϕ, ψ, and Υ families),
The curves show gaps calculated
using the Cornell potential for
quark masses 0.5,1.0,1.5,...,5GeV
left to right. Horizontal dashed lines
and small red circles
indicate calculated values for
successive charmonium states.
extra several states must be tetraquarks